Kinetics of vacancy diffusion on Si(111) surfaces studied by scanning reflection electron microscopy

Heiji Watanabe and Masakazu Ichikawa
Joint Research Center for Atom Technology, Angstrom Technology Partnership (JRCAT-ATP), c/o National Institute for Advanced Interdisciplinary Research, 1-1-4 Higashi, Tsukuba, Ibaraki 305, Japan
(Received 14 March 1996)

The kinetics of vacancy diffusion on Si(111) surfaces is studied by using scanning reflection electron microscopy (SREM). Two types of layer-by-layer etching are observed during low-energy Ar ion irradiation (500 eV) at elevated substrate temperatures. One is step retreat, which is a reversal of step-flow growth, and the other is two-dimensional vacancy island nucleation. These results show that vacancies created by low-energy ion impact diffuse on the surfaces, and are annihilated at the step edges. The vacancy diffusion kinetics on the surfaces are examined by using a SREM technique. An activation energy of 3.0 ± 0.2 eV is obtained from the vacancy diffusion length estimated from the width of the denuded zone, which is created on both sides of the atomic step by thermal heating after vacancy introduction by ion irradiation at room substrate temperature. These results indicate that vacancy diffusion kinetics is dominated by monovacancy formation and diffusion. These processes require thermal excitation to overcome the potential barrier for surface diffusion of adatoms, and to overcome the barrier for lateral binding energy to release adatoms from the step edges. [S0163-1829(96)00432-8]

I. INTRODUCTION

Surface diffusion of adatoms is important in thin-film growth. Because of its technological importance and scientific interest, the kinetics of surface diffusion has been extensively studied by using many kinds of surface analyses, such as reflection high-energy electron diffraction (RHEED) and scanning tunneling microscopy (STM). The relationship between diffusion kinetics and the elementary process of the crystal growth mode has been clarified in detail, especially for semiconductor surfaces. On the other hand, even though etching of semiconductor materials is technologically important for device production, less attention has been paid to clarifying the etching process than to crystal growth. However, there have been several experimental studies of etching in recent years.[1–3] Bedrossian *et al.* demonstrated RHEED intensity oscillation during ion bombardment of Si(100) surfaces by a 250 eV Xe beam;[1] their results suggested layer-by-layer etching behavior, which is typical for crystal growth. They also used STM to investigate anisotropic vacancy annihilation at step edges, based on the directions of dimer rows.[2] Their results suggested that vacancies which are created by low-energy ion impact are mobile, and diffusion kinetics should be dominated by surface structures as well as adatom diffusion. In gaseous etching, RHEED intensity oscillation was also reported for Si(111) surfaces with molecular fluorine by Hiroi and Tatsumi.[3] They also pointed out the possibility of vacancy diffusion for gaseous etching at high substrate temperatures. Recently, Kitamura, Lagally, and Webb investigated thermal diffusion of naturally occurring vacancies on Si(111)-2×1 surfaces in real time using a novel application of STM.[4] By tracing individual vacancy jumps, they successfully measured the activation energy for vacancy diffusion along the dimer rows. Their STM work is valuable and a rare case because it numerically describes vacancy diffusion kinetics. However, the details have not been described experimentally or theoretically.

In this paper, as the most simple and ideal etching, low-energy ion-irradiated Si(111) surfaces are studied by scanning reflection electron microscopy[5,6] (SREM) to investigate the kinetics of surface diffusion of vacancies. We show that the diffusion length of vacancies, which are created by ion impact, dominates layer-by-layer etching. One type of etching is step retreat, which is caused by vacancy annihilation at step edges, observed at around a 900 K substrate temperature. The other is island formation, which is caused by vacancy accumulation on terraces at a low temperature of 900 K. Diffusion constants of surface vacancies at various substrate temperatures are determined by the width of the denuded zone, which is formed on both sides of the atomic step by thermal heating after ion bombardment at room temperature. The kinetics of vacancy diffusion are discussed based on the experimentally obtained activation energy.

II. EXPERIMENT

An ultrahigh-vacuum (UHV) surface analysis system was used.[7] This was equipped with an UHV thermal field emission electron gun (modified Hitachi S-4200 scanning electron microscope) and Ar ion gun. The base pressure of the analysis chamber was 3×10^{-11} Torr. A 30 keV electron beam with a 3 nm diameter and a 0.2 nA current was used for UHV-SREM observation. The diffraction patterns were monitored on a fluorescent screen by a charge-coupled-device camera. The intensity of the diffraction spot was detected by a photo-multiplier with an optical fiber. In this study, SREM images were obtained from a specular reflection spot at $[11\bar{2}]$ incidence and about 3° to the surface.

We used an $11\times2.5\times0.45$ mm^3 specimen, which was cut from a Czochralski-grown (CZ) n-type Si(111) wafer. The

 © 1996 The American Physical Society

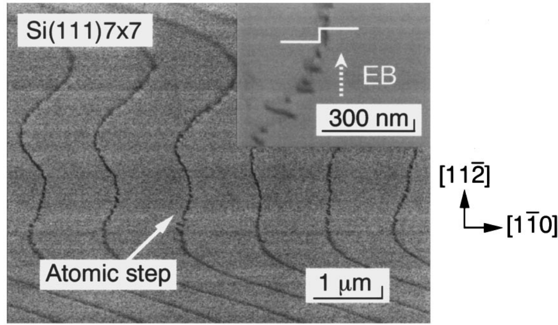

FIG. 1. SREM images of the Si(111)-7×7 clean surface prepared by flash heating. A 30 keV electron beam with a 3 nm diameter and a 0.2 nA current was used for UHV-SREM observation. Each step line corresponds to an atomic step (single biatomic step). A magnified SREM image of the single atomic step is shown in the upper right of the figure. The direction of the incident electron beam is indicated. The step-contrast dependence on the direction of the incident beam shows that the surface becomes lower from right to left.

sample was cleaned by flash heating (at 1400 K for 10 s) after preheating (at 800 K for 20 h) using direct current at UHV conditions of less than 5×10^{-10} Torr. Figure 1 is a SREM image obtained after the cleaning; single atomic steps can clearly be observed, and a typical RHEED pattern showing 7×7 reconstruction appears. Since the SREM image is vertically compressed, the atomic steps running along the [11$\bar{2}$] direction wave gently. As shown in the magnified SREM image in Fig. 1, step roughening naturally occurs depending on the directions of the preferentially formed steps of the surface reconstruction. Based on the step-contrast dependence on the direction of the incident electron beam in the high-resolution SREM image, it is obvious that the surface becomes lower from right to left. Therefore, we can easily determine the step motion to be upward or in the opposite direction simply by using SREM images.

Ar ions with a 500 eV kinetic energy were used for ion sputtering of the Si(111) surfaces. The ion current density and incident angle were 16 nA/cm^2 and 43° to the surface, respectively. The Ar gas pressure in the analysis chamber was kept at 2×10^{-8} Torr during sputtering. We performed two series of experiments to investigate the etching behavior. In the first experiment, Ar ions were irradiated onto the Si(111)-7×7 surfaces at elevated substrate temperatures of 900–1070 K by direct current heating. The substrate temperatures were monitored by using an optical pyrometer. SREM observation was performed after the sample was cooled to room temperature, and the Ar gas was purged. The second experiment was to investigate the diffusion kinetics of the vacancies in detail. The elemental processes of vacancy formation by ion impact and surface diffusion of vacancies occurred at different times. That is, after low-energy ion irradiation onto the Si(111)-7×7 surfaces at room temperature, the sample was heated for a certain period. An electric field during direct current heating affects the diffusion behavior of positively charged adatoms on Si surfaces.[8] Therefore, the sample was heated to 773–1010 K by using a chemical-vapor-deposited pyrolytic boron nitride (PBN)/pyrolytic graphite (PG) ceramics heater. During thermal heating, the vacuum chamber was kept at less than 1×10^{-9} Torr. SREM observation was performed after the sample was cooled to room temperature.

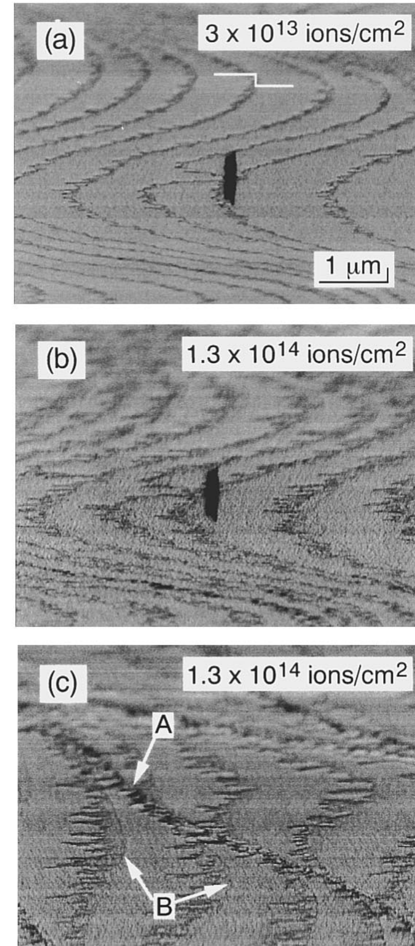

FIG. 2. SREM images of the Si(111) surface after ion sputtering at a 990 K substrate temperature. Ar ions with 500 eV kinetic energy were irradiated onto the Si(111)-7×7 surface. (a) and (b) resulted from ion doses of 3×10^{13} and 1.3×10^{14} ions/cm^2, respectively. (c) shows an area which includes wide terraces and bunched step edges labeled *A* after a 1.3×10^{14} ions/cm^2 ion dose. *B* shows the trace remaining after step retreat by ion sputtering. The sample becomes lower from left to right.

III. RESULTS AND DISCUSSION

A. Observation of the initial stage of layer-by-layer sputtering

Figures 2(a)–2(c) show SREM images of the ion-sputtered Si(111) surfaces. Ar ions were irradiated onto a Si(111)-7×7 reconstructed surface at a substrate temperature of 990 K. After an ion dose of 3×10^{13} ions/cm^2 [Fig. 2(a)], the step edges become rough compared to the clean surfaces (Fig. 1), although no significant change was observed on the terraces in the SREM image. When the ion dose was increased to 1.3×10^{14} ions/cm^2, this step roughening was enhanced [Fig. 2(b)]. For both surfaces, 7×7 RHEED patterns were clearly observed on the terraces. On the other area, which includes wide terraces [Fig. 2(c)], the steps obviously retreated upward after ion irradiation. At the bunched step edges labeled *A*, the step retreat width was less than that for the other single steps. Moreover, we were able

to observe some traces remaining at the point where there were steps before ion irradiation (labeled *B*).

During low-energy ion bombardment, since collisions with the substrate are limited to a few atoms, some of these atoms are ejected from the surface without displacing other atoms.[9,10] STM experiments have shown that low-energy ion irradiation creates atomic-scale pits on semiconductor surfaces without destroying surface reconstruction.[2,11] In our experiment, there was no change in the 7×7 RHEED pattern for the 990 K substrate temperature. This means that although we cannot determine whether a perfect dimer and adatom stacking-fault (DAS) structure remains after ion irradiation, the ion-irradiated Si surface at a 990 K substrate temperature involves strict 7×7 ordering.

There are two possible ways of explaining these experimentally obtained results (step retreat caused by ion irradiation and existence of 7×7 ordering after sputtering at an elevated substrate temperature). One is preferential sputtering at the step edges, and the other is vacancy mobility. However, highly selective sputtering cannot be expected only at step edges with an ion kinetic energy of over a few hundred eV, and the thermal excitation of the surface influences maintenance of 7×7 ordering. Thus we can conclude that vacancies are mobile at this substrate temperature. Therefore, the experimental results are explained as follows. Individual vacancies which are randomly created on terraces by ion impact are mobile, and have enough diffusion length to reach the step edges. Vacancy annihilation at the low step edges causes the steps to move upward. If vacancy annihilation occurs at the upper step edges, the vacancies should be filled up with atoms supplied from the upper steps. For the single steps in Figs. 2(b) and 2(c), assuming a sputtering yield of about 1 atom/ion, the number of atoms estimated to be removed from the ion dose corresponds to 0.1 biatomic layer. This correlates well with the average width of the step retreat. Since vacancies which arrive at the step bands are consumed by each step edge, step roughening and retreat are less than those of the single step, as shown in Fig. 2(c) (indicated by the label *A*). These phenomena can be easily understood as the reverse of the step-flow mode in crystal growth. Considering that the $[\bar{1}\,\bar{1}2]$ steps are preferentially formed on a homoepitaxial Si(111) surface, the zigzag shape of the step edges after ion sputtering may be induced by the crystal orientation. In the local area, it is presumed that surface reconstruction is repaired by thermal vacancy diffusion during ion irradiation. However, since we quenched the sample surface after ion sputtering for stable SREM observation, the slight constrast change on terraces, especially for high ion doses [Figs. 2(b) and 2(c)], can be attributed to the frozen vacancies remaining on the terraces. Moreover, since complicated bond rearrangement is required for filling up vacancies at the upper step edges, a possible cause of the origin of the traces left on the terrace [labeled *B* in Fig. 2(c)] is discontinuities, including vacancy chains which are accidentally formed without being filled up with the atoms from the upper step edges. A similar phenomenon will be discussed in Sec. III B.

At a higher temperature of 1070 K, the step edges become smooth. This means that thermal enhancement of vacancy diffusion shortened and smoothed the step edges, thereby minimizing surface energy.[12] However, at a high temperature, many SiC particles were formed on the terraces, because of reactions between the surfaces and hydrocarbons, which were contained with the Ar gas for sputtering or which were caused by ion bombardment of the chamber wall.

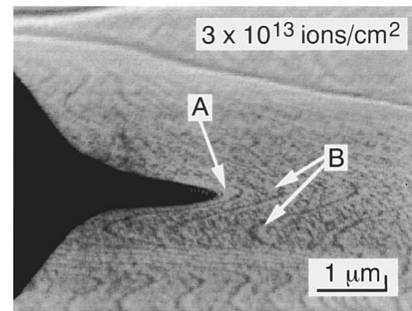

FIG. 3. Results of 500 eV Ar ion irradiation at a dose of 3×10^{13} ions/cm^2 at a 900 K substrate temperature. There are many dark contrast spots on the terraces. At the areas labeled *A* and *B*, there are few dark spots. The dark constrast area on the left side is a large SiC particle formed during sample preparation. The sample becomes lower from left to right.

Figure 3 shows a SREM image of the Si(111) surfaces after ion-beam irradiation at 3×10^{13} ions/cm^2 at a substrate temperature of 900 K. Although a 7×7 RHEED pattern can also be recognized on this surface, the features of the ion-irradiated surface are different from the results at a 990 K substrate temperature (Fig. 2). That is, there are many dark spots that are less 50 nm in diameter, and the step lines become slightly broader than those of clean surfaces. There are few dark spots on the narrow terraces (labeled *A*) and near the steps (labeled *B*).

Based on the thermal diffusion of vacancies, these results suggest that not all vacancies created on the terraces could reach the step edges, because thermal diffusion is suppressed at this low temperature. This causes nucleation of ''vacancy islands,'' which are observed as dark spots in the SREM image (Fig. 3). The formation of vacancy islands with a single-layer depth after ion irradiation at elevated substrate temperatures has also been reported for Si(100) and GaAs(110) surfaces in previous STM studies.[2,11] Our SREM results correlated well with these STM studies. This means that the outermost atoms are periodically removed by two-dimensional vacancy island nucleation. This etching behavior is also similar to layer-by-layer crystal growth. RHEED intensity oscillation during ion sputtering reported for Si(100) surfaces by Bedrossian *et al.*[1] will take place on Si(111) surfaces at this substrate temperature. Note that the denuded zones, which include almost no vacancy islands, are created at the terrace edges (labels *A* and *B*). The depletion of vacancy islands in the denuded zone means vacancy annihilation near the step edges. This process explains the slight broadening of the step lines in the SREM image (Fig. 3). Details of vacancy diffusion kinetics mediated by two-dimensional island nucleation will be discussed in Sec. III C.

B. Measuring the vacancy diffusion constant and activation barrier

The simultaneous ion sputtering at elevated substrate temperatures described in the preceding section showed that

etching behavior with low-energy ions has many similarities to homoepitaxial film growth. This process is characterized by a reversal of the step-flow mode at high temperatures, and two-dimensional island nucleation at moderate temperatures. In both cases, vacancies are created and diffused simultaneously. Surface amorphization was observed only with certain conditions at a low substrate temperature. Clearly, these changes in the etching mode are affected by the substrate temperatures. Although we are not sure that the kinetic energy of Ar ions at 500 eV is low enough for continuous layer-by-layer etching, we observed the initial stage of the layer-by-layer etching behavior. Therefore, we estimated the diffusion kinetics of vacancies from SREM observation.

Recently, Doi and Ichikawa reported SREM studies that characterized diffusion of adatoms on a Si(100) surface.[13–15] They estimated the diffusion length of adatoms by measuring the width of the denuded zone formed during a certain period of thermal heating after Si atom deposition. Here, we introduced vacancies on the Si(111)-7×7 surfaces by low-energy ion sputtering and then the samples were heated with a ceramic heater. Figure 4(a) shows the Si(111) surface after ion sputtering with a dose of 5×10^{13} ions/cm^2 at room substrate temperature. Because the diffraction intensity of the specular spot becomes weak, the SREM contrast between steps and terraces is less than that of clean surfaces. The RHEED pattern showing 7×7 ordering could hardly be observed on the fluorescent screen. However, there was no change in the shape of the step lines in the SREM image. This means that individual vacancies are frozen without diffusion on the surface.

Figures 4(b), 4(c), and 4(d) show the results of thermal heating at 971 K after ion irradiation with annealing periods of 3, 7, and 20 min, respectively. The 7×7 RHEED pattern was observed from these surfaces. In these SREM images, we clearly recognized the formation of dark spots on the terraces, as well as the creation of a denuded zone. High-resolution SREM images of the large dark spots on terraces which grew after a long annealing period showed that these spots correspond to vacancy islands with a single atomic depth. The surface morphology is schematically illustrated in Fig. 4(e). This appearance is consistent with the results of simultaneous ion sputtering at a 900 K substrate temperature (Fig. 3). For simultaneous sputtering at high substrate temperatures, the energetic beam should enhance vacancy diffusion, as reported for film growth.[16] However, the changes observed in Figs. 4(b)–4(d) can be attributed only to the thermal effect. In Fig. 4(b), there are many vacancy islands of about 30 nm in diameter in the middle of the terraces. When the annealing time is increased, the vacancy islands become large and the mean distance between them increases [Figs. 4(c) and 4(d)]. With an annealing time of several minutes, large vacancy islands (''vacancy pits'') are formed on the step edges. We think that these large pits are formed when the vacancies, which arrive from the lower terrace, are not accidentally filed up with adatoms from the upper step edges. Since these vacancy pits have a discontinuity of a single atomic height from the lower terrace, and a double atomic height to the upper terrace, they act as a sink for vacancy annihilation instead of acting as naturally formed steps on the surfaces. For these vacancy pits, the steps which face the lower terraces retreat downward. Therefore, vacancy pits grow, as shown in the SREM images. These results are similar to the trace remaining on the terraces after ion irradiation at 990 K [Fig. 2(c)]. Moreover, considering the vertical compression of the SREM image, these vacancy pits have circular shapes. Although anisotropic diffusion and annihilation both for adatoms and vacancies have been reported for Si(100) surfaces,[2,17] this result suggests that the Si(111) surface is isotropic for vacancy diffusion.

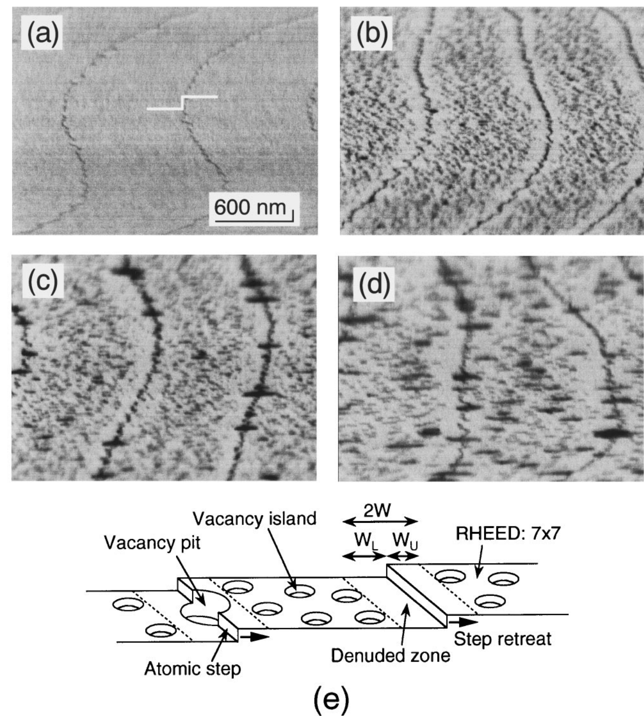

FIG. 4. The formation and diffusion processes of vacancy islands on the Si(111) surface during thermal heating at 971 K. Vacancies were introduced on the Si(111)-7×7 surface by low-energy Ar ions with a dose of 5×10^{13} ions/cm^2 at room substrate temperature. (a) shows the ion-irradiated surface. Although the deflection intensity was weakened after sputtering, there is no change in the shape of the step lines. (b)–(d) show thermal heating results with periods of 3, 7, and 20 min, respectively. The dark spots on the terraces correspond to vacancy islands created by the accumulation of monovacancies. In SREM images (b)–(d), denuded zones, which include no vacancy islands, are observed along the step edges. With an increase in heating time, ''vacancy pits'' were formed at the step edges. (e) shows a schematic illustration of the surface morphology. The vacancy diffusion length (x) can be estimated from the width of the denuded zones (W). The sample becomes lower from right to left.

If vacancies which arrive at step edges are annihilated without a larger energy barrier than that of the surface diffusion, we can estimate the diffusion length of surface vacancies by measuring the width of the denuded zone formed after thermal heating. We measured the width of the denuded zone as a function of heating time in the temperature range from 773 to 1010 K. Since vacancy annihilation causes step retreat, the width of the denuded zone is not the same on both sides of the step lines, as illustrated in Fig. 4(e) ($W_L > W_U$). Therefore, we defined the vacancy diffusion length (x) to be half the sum of the width of the denuded

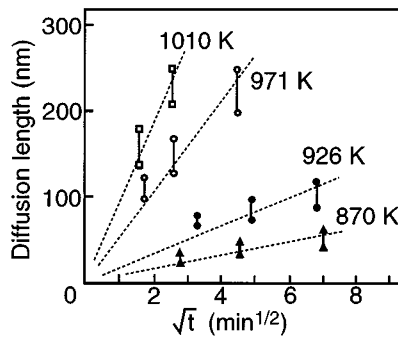

FIG. 5. Vacancy diffusion length at 870–1010 K annealing temperatures is shown as a function of the square root of the heating time. The diffusion length is proportional to the square root of the annealing time at each temperature. With thermal heating at 773 K for 22 min, we could not observe the denuded zone from the SREM images.

zones next to the step edges (W). This procedure for estimation of the diffusion length can be used only in the case of low vacancy density (about 0.03 ML of vacancies are thought to be introduced onto the surface by low-energy ion sputtering). Figure 5 shows the diffusion length ($x=W$) as a function of the square root of the annealing time. The results suggest that the diffusion length of vacancies is proportional to the square root of the annealing time at temperatures of 870–1010 K, and that vacancy diffusion is dominated by Brownian motion. The diffusion constant D is given by the relationship between annealing time t and diffusion length x as $D=x^2/t$. For example, the diffusion constant of the vacancies was calculated to be $(1.1-1.6)\times 10^{-12}$ cm^2/s at 1010 K. This value is one or two orders less than that of adatom diffusion on Si(100)-2×1 and 1×2 surfaces at 1023 K.[15] At 773 K,we could not observe formation of a denuded zone or a 7×7 RHEED pattern, even after 22 min of annealing. This means that the diffusion length of vacancies is less than the size of the unit cell of the 7×7 reconstruction. Arrhenius plots of these results are shown in Fig. 6. The diffusion constants for 870–1010 K fit well with the dotted line. This line also explains the result at 773 K. The activation energy for the vacancy diffusion was 3.0 ± 0.2 eV.

C. Model of surface vacancy diffusion and its kinetics

For crystal growth, we consider the motion of adsorbates to analyze the growth kinetics. The activation energy of Si

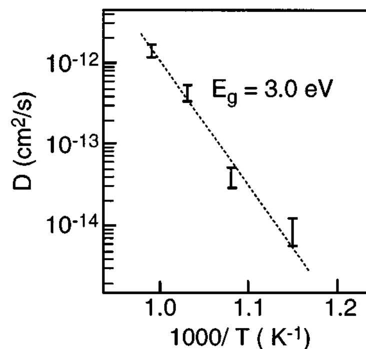

FIG. 6. Arrhenius plots for vacancy diffusion length estimated from the width of the denuded zone. An activation energy of 3.0 ± 0.2 eV was obtained for vacancy diffusion on the Si(111) surface.

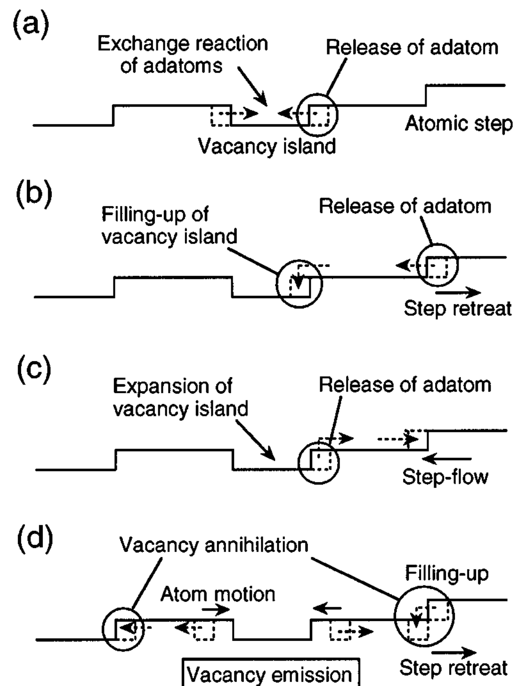

FIG. 7. Schematic illustrations of potential models for surface processes. (a) shows the release of adatoms from the step edges of vacancy islands. (b) shows adatom transfer from naturally existing steps to vacancy islands. (c) shows adatom transfer from step edges of vacancy islands to the upper terraces. (d) shows vacancy emission from step edges of the islands and vacancy diffusion on terraces. Model (d) successfully explains our experimental results.

adsorbate diffusion on Si(111)-7×7 surfaces has been experimentally obtained to be around 1.3 eV.[6,18] However, the vacancy diffusion process is more complicated because we must consider the following elemental processes. At the initial stage of thermal annealing, monovacancies or small vacancy clusters with a few unit cells introduced on the surfaces gather, and vacancy islands are formed on the terraces. After these islands grow over a few nanometers in diameter, we can recognize the presence of these islands as dark spots in SREM images. Therefore, in the initial heating stage, it is enough to consider the monovacancy diffusion to describe the experimental results. Then, the vacancy islands near the step edges seem to move away from the steps, and this process creates a denuded zone along the steps. Here, we must discuss possible processes which allow vacancy island motion. Figures 7(a)–7(d) show potential models for the surface processes. If adatom monomers are created by the release of Si atoms from the steps of the vacancy islands [Fig. 7(a)], these adatoms can easily move inside the vacancy islands due to the relatively low activation energy for surface diffusion. However, since there is no adatom density gradient, the exchange reaction of adatoms within the vacancy islands does not allow long-range island motion, and this reaction cannot explain changes in island diameters. Thus, there are two possible processes to explain experimental results. One is adatom transfer between steps of vacancy islands and naturally existing steps. The other is actual movement of vacancy islands mediated by monovacancy formation and diffusion. If adatoms are supplied from the naturally existing step edges [Fig. 7(b)], the formation of the denuded zone can

be interpreted as step retreat caused by adatom release and their thermal diffusion from the steps. However, since this process always fills up vacancy islands, expansion of vacancy islands is not allowed. This means that the changes in island diameters cannot be explained unless we introduce a supply of adatoms from the step edges of vacancy islands to the upper terraces [Fig. 7(c)]. In this case, although the changes in island diameters are explained, the step retreat process and the formation of denuded zones observed in Figs. 2 and 4 are not satisfied, and a complicated bond rearrangement is required. Thus, we believe that the motion of the vacancy islands must be caused by anisotropic emission of monovacancies outside the vacancy islands [Fig. 7(d)]. That is, when monovacancies are annihilated at naturally existing step edges, a selective emission of monovacancies takes place at the side of the step edges of vacancy islands neighboring initially existing step edges. The selective emission is driven by the density gradient of vacancies on terraces. To create monovacancies, Si atoms at the step edges must go forward inside the vacancy islands. This result in vacancy island motion away from the naturally existing steps. Moreover, the expansion of vacancy islands takes place by vacancy supply from neighboring islands and by gathering of vacancy islands. Therefore, we can conclude that an elemental process involved in our experiments is monovacancy creation and diffusion in any stage.

For the motion of monovacancies, the Si atoms next to the monovacancies must move in the opposite direction. This process should go across two kinds of potential barriers; one is the formation energy of adatoms, which is equal to lateral bond breaking; the other is surface diffusion of adatoms themselves. In the case of monovacancy creation, a similar bond rearrangement must occur at the step edges. As a result, the diffusion constant D is

$$D = A \exp[-(E_s + E_b + E_{SW})/kT],$$

where A, E_s, E_b, E_{SW}, and T are the frequency factor, the activation energy for surface diffusion of adatoms, the lateral binding energy of Si atoms at step edges, the Schwoebel barrier energy, and the substrate temperature. The relation is similar to the model which has been used to describe the surface diffusion of adatoms and two-dimensional nucleation on a homoepitaxial surface.[19] Surface diffusion of monomer adatoms can be described by substituting $E_b = 0$ eV into the equation. Assuming a simple surface which does not show the Schwoebel effect, the growth mode is dominated only by monomer diffusion $[D = A \exp(-E_s/kT)]$. This describes the step-flow mode of crystal growth observed in the case of a low flux rate and adsorbates with enough diffusion length. When we discuss two-dimensional nucleation, we must consider the dissociation process of two-dimensional adatom islands in creating monomers. In the case of monovacancy diffusion on terraces, because the movement of Si atoms next to the vacancies can be treated as a release of adatoms from two-dimensional clusters, we believe that the energy barrier of E_b for vacancy diffusion is equal to that for homoepitaxial Si(111) surfaces. Moreover, since the ratio between the widths of neighboring denuded zones (W_L/W_U) can be explained by the step retreat caused by the vacancy annihilation (Fig. 4), E_{SW} is though to be negligible. For the two-dimensional island growth mode on Si(111) surfaces, the E_b value of 1.6 eV agrees well with Monte Carlo simulation and experimental results.[19] Although the details of the potential barrier for surface vacancy migration related to the 7×7 unit cell, such as corner holes and dimers, are not clarified from our SREM study, the macroscopic activation energies obtained from the Si homoepitaxial surfaces can be applied to the vacancy diffusion. With these results ($E_s = 1.3$ eV, $E_b = 1.6$ eV, $E_{SW} = 0$ eV), the activation energy of monovacancy diffusion ($E_s + E_b + E_{SW}$) is estimated to be 2.9 eV, which coincides well with our results.

In previous studies, the activation energy of adatom diffusion was estimated to be around 3.0 eV,[18,20] and the Schwoebel effect was not observed for Si(111) surfaces mediated by two-dimensional nucleation. These results show that even though these processes are dominated by different mediations (vacancy diffusion and adatom diffusion), the elementary processes which determine their kinetics are apparently similar. However, the diffusion constants of adatoms and vacancies must be different. This is because, after the Si atoms are released from the step edges, they can easily diffuse on the surface with an activation energy of about 1.3 eV. On the other had, monovacancy diffusion must overcome the high energy barrier in each motion equal to the lattice constant. Therefore, the frequency factor and the diffusion constant of the vacancy should be less than those of adatoms. This prediction can explain the two orders of magnitude difference in diffusion constants between our results and previous work reported by Doi *et al.* for adatom diffusion on Si(100) surfaces.

IV. CONCLUSION

We have investigated diffusion kinetics of surface vacancies on Si(111) surfaces by SREM. Layer-by-layer sputtering using low-energy Ar ions was characterized by a reversal of the step-flow mode and two-dimensional vacancy island nucleation. In both cases, the thermal diffusion of monovacancies and the vacancy annihilation at step edges were elementary processes. The diffusion length of the vacancies was estimated from the width of the denuded zone created along the step edges by the thermal heating after vacancy formation at room substrate temperature. The activation energy for vacancy diffusion was 3.0 eV. We propose that vacancy diffusion kinetics is dominated by monovacancy diffusion, which requires thermal excitation for surface diffusion of adatoms and lateral bond breaking to release adatoms from the steps.

ACKNOWLEDGMENTS

This work, partly supported by NEDO, was performed at the Joint Research Center for Atom Technology (JRCAT) under the joint research agreement between the National Institute for Advanced Interdisciplinary Research (NAIR) and the Angstrom Technology Partnership (ATP).

[1] P. Bedrossian, J. E. Houston, J. Y. Tsao, E. Chason, and S. T. Picraux, Phys. Rev. Lett. **67**, 124 (1991).
[2] P. Bedrossian and T. Klitsner, Phys. Rev. Lett. **68**, 646 (1992).
[3] M. Hiroi and T. Tatsumi, Jpn. J. Appl. Phys. **33**, 2244 (1994).
[4] N. Kitamura, M. G. Lagally, and M. B. Webb, Phys. Rev. Lett. **71**, 2082 (1993).
[5] M. Ichikawa, T. Doi, M. Ichihashi, and K. Hayakawa, Jpn. J. Appl. Phys. **23**, 913 (1984).
[6] M. Ichikawa and T. Doi, in *Reflection High Energy Electron Diffraction and Reflection Electron Imaging of Surfaces*, Vol. 188 of *NATO Advanced Science Institute, Series B: Physics,* edited by P. K. Larsen and P. J. Dobson (Plenum, New York, 1988), p. 343.
[7] H. Watanabe and M. Ichikawa (unpublished).
[8] A. V. Latyshev, A. B. Krasilmikov, A. L. Aseev, and S. I. Stenin, JETP Lett. **48**, 529 (1988).
[9] J. Y. Tsao, E. Chason, K. Horn, D. Brice, and S. T. Picraux, Nucl. Instrum. Methods Phys. Res. Sect. B **39**, 72 (1989).
[10] M. Robinson, in *Sputtering by Particle Bombardment 1*, edited by R. Behrisch (Springer, Berlin, 1981), p. 73.
[11] X.-S. Wang, R. J. Pechman, J. H. Weaver, Appl. Phys. Lett. **65**, 2818 (1994).
[12] H. Watanabe and M. Ichikawa, Appl. Phys. Lett. **68**, 2514 (1996).
[13] T. Doi and M. Ichikawa, Jpn. J. Appl. Phys. **34**, 25 (1995).
[14] T. Doi and M. Ichikawa, Jpn. J. Appl. Phys. **34** 3637 (1995).
[15] T. Doi, M. Ichikawa, S. Hosoki, and K. Ninomiya, Surf. Sci. **343**, 24 (1995).
[16] N.-E. Lee, G. A. Tomasch, and J. E. Greene, Appl. Phys. Lett. **65**, 3236 (1994).
[17] Y.-W. Mo and M. G. Lagally, Surf. Sci. **248**, 313 (1991).
[18] A. V. Latyshev, A. B. Krasilnikov, and A. L. Aseev, Phys. Status Solidi A **146**, 251 (1994).
[19] H. Nakahara, M. Ichikawa, and S. Stoyanov, Surf. Sci. **329**, 115 (1995).
[20] H. Nakahara and M. Ichikawa, Appl. Phys. Lett. **61**, 1531 (1992).